

Mémoire de Maîtrise en médecine No 2395

---

# **Neoangiogenesis assessment in gliomas with $^{68}\text{Ga}$ -NODAGA-RGD PET and IVIM MR Imaging – a pilot study.**

---

## ***Etudiant***

Rami Hajri

## ***Tuteur***

Prof. John Prior, PhD MD  
Chef de service  
Médecine nucléaire et imagerie  
moléculaire, CHUV

## ***Co-tuteur***

Prof. Philippe Maeder  
Professeur associé  
Radiodiagnostic et radiologie  
interventionnelle, CHUV

## ***Expert***

Dr. Patric Hagmann, PD MER  
Radiodiagnostic et radiologie  
interventionnelle, CHUV

Lausanne, le 15 décembre 2015

## ABSTRACT

Background and purpose: Recent development of anti-angiogenic drugs in oncology without any direct marker of angiogenesis has lead to the elaboration of a new PET tracer referred as  $^{68}\text{Ga}$ -NODAGA-RGD. This radiotracer consists of a sequence of three amino acids abbreviated RGD and has the capacity to bind to  $\alpha_v\beta_3$  integrins present tumoral vessels. We evaluate this new tracer in the framework of tumoral angiogenesis in native gliomas. The aim of this study is to describe the distribution of the tracer compared to  $^{18}\text{F}$ -FET PET that highlights tumor protein transport and to IVIM MRI that highlights micro-perfusion. Long-term work consists of determining whether RGD tracer could allow a better selection of patients who could benefit from an anti-angiogenic treatment and an earlier assessment of response to treatment.

Materials and methods: Two patients were included in this study. A qualitative analysis of the tracer uptake compared to  $^{18}\text{F}$ -FET PET and IVIM MRI was realized.

Results: Our first patient had a bi-component glioblastoma/high-grade glioma with an anterior part corresponding to a WHO grade IV glioblastoma and a posterior part to a high-grade glioma. RGD was only taken up by the glioblastoma part whereas  $^{18}\text{F}$ -FET was taken up by both parts. The comparison with IVIM showed no correlation in this patient. The second patient with a WHO grade II ganglioglioma showed no RGD uptake, no IVIM signal but a high  $^{18}\text{F}$ -FET uptake by the whole tumor.

Conclusions: RGD uptake shows a different process than  $^{18}\text{F}$ -FET PET and IVIM MRI in gliomas in two patients. This needs to be further examined in a larger cohort to consolidate our interesting preliminary results.

Key words: angiogenesis-gliomas-RGD-IVIM-integrins.

## **ACKNOWLEDGEMENTS**

I would like to address special thanks to Pr. Johannes Czernin and Dr. Ken Herrmann who supervised me during my elective in the Department of molecular, medical pharmacology and nuclear medicine clinic in UCLA and who aroused my interest in medical imaging.

Many thanks to Pr. Maeder, who provided the MR images analysis and Dr. Hagmann, who was the expert for this work. Thanks as well to Dr. Vincent Dunet, who helped me throughout the whole procedure with great support and clear advices.

Thanks to Dr. Rossella Sarro and Dr. Jean-Philippe Brouland, who provided the histopathological results and analysis for the correlation with our images.

Of course I am very thankful towards my supervisor Pr. John Prior, who gave me the opportunity to select a topic and to do an internship abroad in his domain. I would like to thank him also for his limitless availability, his clear-sighted advice and for keeping faith throughout the difficulties of getting patients.

## CONTENTS

<b>INTRODUCTION</b>	<b>1</b>
<b>METHODOLOGY</b>	<b>5</b>
<b>RESULTS</b>	<b>8</b>
<b>DISCUSSION</b>	<b>13</b>
<b>BIBLIOGRAPHY</b>	<b>20</b>

# INTRODUCTION

The formation of new vessels, a process also known as neoangiogenesis is one of the fundamental pathophysiological mechanisms for the development and proliferation of cancer. Tumoral cells need nutrients and oxygen for their development that normal tissue vasculature cannot afford. Thus, in order to fulfill their needs, tumoral cells secrete pro-angiogenic growth factors that act on endothelial cells and their environment to stimulate the formation of new vessels (1). Neoangiogenesis implies two main signal proteins pathways referred as Vascular Endothelial Growth Factor-A (VEGF-A) and integrins (2) (3).

Integrins are cell surface heterodimeric glycoproteins, consistent of an  $\alpha$  and  $\beta$  subunit, that allow cell adhesion, migration, proliferation and differentiation on normal and tumoral blood vessels. Among the integrin family, some of them such as  $\alpha_v\beta_3$  are implicated in cancer angiogenesis, invasion and metastasis. It is a fundamental process in tumor growth and in development of resistance to chemotherapy and radiation therapy, which therefore consists on a promising target (4) (5).

$\alpha_v\beta_3$  is one of the most studied type of integrin in cancer.  $\alpha_v\beta_3$  is preferentially expressed on tumoral endothelial cells to facilitate the growth and survival of the newly forming vessels (6) (7). However they are not overexpressed in quiescent endothelium. This characteristic makes it an interesting target for antiangiogenic therapy and angiogenesis imaging marker (8) (9) (10) (11).

So far there is no direct marker of angiogenesis thus, a molecular PET imaging probe has been developed with a sequence of three amino-acids : arginine-glycine-aspartic acid, abbreviated RGD and has the capacity to bind to  $\alpha_v\beta_3$  integrins (12) (13) (14) (15).

Based on the understanding of these cellular pathways, the recent development of new oncologic tools for the treatment of tumors, including brain tumors has lead to the creation of anti-angiogenic treatments that target VEGF-A receptor (*bevacizumab*) and integrins (*cilengitide*). *Cilengitide* is currently under clinical investigation (4).

Bevacizumab is a humanized monoclonal antibody that inhibits the effect of VEGF-A and induces a decrease in microvasculature and a return to baseline of the remaining capillaries on a functional and architectural plan (16).

Before starting a specific treatment, it remains difficult to evaluate neoangiogenesis phenomenon, to evaluate early response to an anti-angiogenic treatment and to differentiate between relapse and radio-necrosis on conventional imaging (17) (18) (19). PET-MR image fusion has the potential to obtain a non-invasive characterization of tumoral angiogenesis either with PET tracers targeting integrins on neovessels or by indirect measure of tumoral perfusion (20) (21) (22) (23). So far, several PET tracers allow an assessment of tumoral cell proliferation before and during treatment with their glucose metabolism (FDG) or protein transport (FET), but they do not measure angiogenesis phenomenon (24) .

<sup>18</sup>F-fluoroethyltyrosine (FET) is an artificial amino acid, which is taken up into upregulated cancerous cells. Therefore FET gives information about tumor metabolism of proteins (25). FET can be used to provide the best site for biopsy in heterogeneous tumors and to diagnose early residual tumor after resection (26) (27) (28) (29).

The microvasculature changes induced by anti-angiogenic treatments occur before the morphological changes detectable by conventional imaging such as MR (30). There is a need to evaluate the targets before starting a treatment and an early detection of response or non-response to the treatment during treatment follow-up (31). Thus, a specific molecular probe that targets neoangiogenesis is needed.

In this study neoangiogenesis phenomenon are assessed in the context of gliomas. Primary brain tumors represent 1-2% of adult cancers. Gliomas are the most common (80%) malignant primary brain tumor (32). According to the classification of the World Health Organization (WHO), there are 3 main types of gliomas: oligodendrogliomas, astrocytomas and mixed oligoastrocytomas (33).

They are divided into two types of grades with different prognosis and approaches: grade I and II are considered as low-grade with a slow-moving evolution and grade III (anaplastic) and IV (glioblastoma) are considered as high-grade with a very short evolution leading to death if untreated (34) (35).

An estimated 68'480 new cases of primary central nervous system tumors are expected to be diagnosed in the United States in 2015 according to the Central Brain Tumor Registry of the United States of primary brain tumors

(36), of which an estimated 23'180 new cases will be malignant (37). With a poor 5-year survival rate after diagnosis of about 17.7% in patients aged of 55-64 years old, this percentage reaches 5.9% in patients aged more than 75 years old. They remain unfortunately incurable for the majority of them because of late diagnosis and poor variety of treatments.

MRI T<sub>1</sub>, T<sub>2</sub> and gadolinium-enhanced sequences play a key role in initial diagnosis and follow-up because of obvious high structural resolution (38). However MRI lacks specificity especially after treatment where for example contrast enhancement reflects a non-specific increased permeability of blood-brain barrier (39) (31).

The high heterogeneity of gliomas composition and irregular shapes make the assessment of response to treatment difficult especially with criteria of linear measurements of enhancing tumor components (40). This limits the interpretation of MRI even by experienced radiologists and consequently makes it difficult to provide the information about the best site to biopsy in particular when there is no contrast enhancement (41).

In addition to that, in 1988 Le Bihan et al. (42) defined intravoxel incoherent motion (IVIM) as a new technique of cerebral perfusion measurement that uses a diffusion sequence with several b-values and a bi-compartmental model to measure blood pseudo-diffusion caused by its passage through microvasculature (43) (44) (45). IVIM measures microscopic translational motions that occur in each image voxel during an MRI acquisition. In biological tissues, these motions are due to microcirculation of the blood in the capillary network and to molecular diffusion of water. These two phenomena constitute the bi-exponential decay of the observed signal on diffusion-weighted images (DWI) when several diffusion b-values are employed (46) (47) (48).

This method allows us to evaluate quantitatively the tumoral capillary microcirculation. IVIM has shown promising results to help differentiate between high- and low-grade tumors, such as in the salivary gland, pancreas, renal, breast. In brain, the IVIM perfusion fraction might be a good tool to differentiate between high- and low-grade gliomas, but is still under clinical investigation (37) (49).

Dynamic susceptibility contrast (DSC) is the usual technique used to measure cerebral perfusion on MRI. It is sensible to neoangiogenesis and is part of all the investigation protocols and brain tumors follow-ups. The latter will be used as a reference for the IVIM technique (50) (51) (52).

Furthermore,  $^{18}\text{F}$ -FDG PET is commonly used to assess malignant disease and treatment response in several organs such as lungs, breasts, lymph nodes, and melanomas. Nevertheless  $^{18}\text{F}$ -FDG shows normal uptake within normal brain and brain inflammation, which makes it unreliable for assessing malignancy in brain particularly for low-grade tumors (53).

Current treatment for gliomas involves surgery, chemotherapy with temozolomide and radiation therapy. In case of recurrent disease after first line treatment, an anti-angiogenic treatment such as bevacizumab is usually given according to the guidelines (54).

A new radiotracer that represents a tool to assess neoangiogenesis is  $^{68}\text{Ga}$ -NODAGA-RGD, which binds to  $\alpha_v\beta_3$  integrins located on the surface of endothelium and macrophages present on neovessels (55) (56) (57).

The clinical applications of RGD for gliomas will be a better characterization of cancerous lesions (58) and a better quantification of neovessels. Moreover, it could provide a more appropriate selection of patients who will benefit from an angiogenesis inhibitor, an earlier assessment of response to angiogenesis inhibitor (59), a more accurate way to monitor therapy and a better characterization of recurrent disease especially after radiotherapy. Consequently, in the long term RGD could improve the diagnostic and the choice of an anti-angiogenic treatment and the follow-up patients could benefit from.

The existence of a relationship between tumoral metabolism and neoangiogenesis using PET tracers targeting each function remains to be demonstrated. The same applies to the existence of a relationship between perfusion quantified by IVIM and neoangiogenesis estimated by  $^{68}\text{Ga}$ -NODAGA-RGD, their respective benefits are unknown.

The aim of this study is to demonstrate whether IVIM and  $^{68}\text{Ga}$ -NODAGA-RGD PET measure the same phenomenon and whether a correlation exists with protein metabolism shown with FET PET. We wanted to demonstrate the respective contributions of each technique. As we have the biopsy histopathology report to correlate with the images, we wanted to see whether we could extrapolate information non-invasively from the scans.



# METHODOLOGY

## Study design

Between July 2014 and October 2015, 2 patients (2 men, aged 49 and 68 years, respectively) followed by Dr. Jocelyne Bloch from the Department of Neurosurgery for whom an  $^{18}\text{F}$ -FET PET was indicated to assess the initial extension or a relapse suspicion of a glioma, were offered a  $^{68}\text{Ga}$ -NODAGA-RGD PET to assess the neoangiogenesis phenomenon.

Patients had a preoperative MR imaging examination with  $T_1$ -weighted,  $T_2$ -weighted,  $T_1$ -weighted post-gadolinium sequences (gadoteric acid, Dotarem, Guerbet, Switzerland; 0.1 mmol/kg), diffusion DTI and ADC, DSC perfusion, IVIM and followed by a FET PET and a  $^{68}\text{Ga}$ -NODAGA-RGD within 1 week (except the FET PET of patient 2 that was fused to a previous MRI realized 18 weeks before).

The local ethics committee at University of Lausanne approved the protocol. Each participant gave written informed consent before inclusion.

## Inclusion criteria

Patients had to be less than 85 years old and present a Karnofsky Performance Status of  $\geq 80\%$ .

## Exclusion criteria

Lack of discernment, pregnancy, breastfeeding and aged less than 18 years old.

## **Data acquisition**

### **PET protocol**

Both  $^{18}\text{F}$ -FET-PET and  $^{68}\text{Ga}$ -NODAGA-RGD-PET acquisitions were realized on PET/CT scanner (Discovery D690 TOF, GE Healthcare, Milwaukee, Michigan, USA). All patients fasted for at least 4 hours prior the tracer injection as recommended by European Association of Nuclear Medicine (EANM) guidelines (60)(38).

#### **$^{18}\text{F}$ -FET-PET acquisitions**

A 60-minute acquisition, centered on the skull is performed after an intravenous infusion of 200MBq of  $^{18}\text{F}$ -FET. A low dose CT-Scan is performed to correct the attenuation and for co-registration of images.

#### **$^{68}\text{Ga}$ -NODAGA-RGD-PET acquisitions**

A 60-minute acquisition, centered on the skull is performed after an intravenous infusion of 200MBq of  $^{68}\text{Ga}$ -NODAGA-RGD. A low dose CT-Scan is performed to correct attenuation and for co-registration of images.

### **MRI protocol**

Conventional MR imaging, DSC and IVIM were realized during the same procedure to permit direct comparison. The images were acquired on a 3T MR imaging scanner (Verio, Siemens, Erlangen, Germany), equipped with 32 multi-channel receiver head coils. Before the data acquisition, an 18- to 20-ga needle was inserted in the right or left antecubital vein.

#### **Conventional MRI protocol**

MR images included sagittal  $T_1$ -weighted spin echo, axial  $T_2$ -weighted spin echo and contrast enhanced axial  $T_1$ -weighted spin echo. Diffusion weighted imaging (DWI) or diffusion tensor imaging (DTI) sequences were also performed. DWI was performed by using DWI pulse sequence at  $b = 0 \text{ s} / \text{mm}^2$  and three orthogonal diffusion weighted acquisitions at  $b = 1000 \text{ sec} / \text{mm}^2$ . ADCs being calculated from the trace images. DTI was performed by using 6-30 direction DTI sequence at  $b = 0 \text{ s} / \text{mm}^2$  from which ADCs were calculated.

## **IVIM MR Imaging**

A Stejskal-Tanner diffusion-weighted spin-echo EPI pulse sequence was performed, with several b-values (0, 10, 20, 40, 80, 110, 140, 170, 200, 300, 400, 500, 600, 700, 800, 900 s/mm<sup>2</sup>) in 3 orthogonal directions, and the corresponding trace was calculated.

The images were axially oriented with a section thickness of 4mm, a field of view (FOV) of 297 x 297 mm<sup>2</sup> and a matrix size of 256 x 256 yielding an in-plane resolution of 1.2 x 1.2 mm<sup>2</sup>. Parallel imaging, with an acceleration factor of 2 and a 75% partial Fourier encoding, allowed TR/TE = 4000/99ms. Receiver bandwidth was 1086 Hz/pixel and fat was suppressed with a spectrally selective saturation routine (37).

# RESULTS

2 patients were included in this study. Both underwent surgical stereotaxic tumor biopsy and resection in order to obtain a histological classification according to the World Health Organization classification of the tumors of the central nervous system and the 3<sup>rd</sup> edition of the International Classification of Diseases for Oncology (ICD-O-3). The pathologists were blinded for imaging results.

We reviewed the histopathological slices with two pathologists and correlated them to our images.

## **Patient 1:**

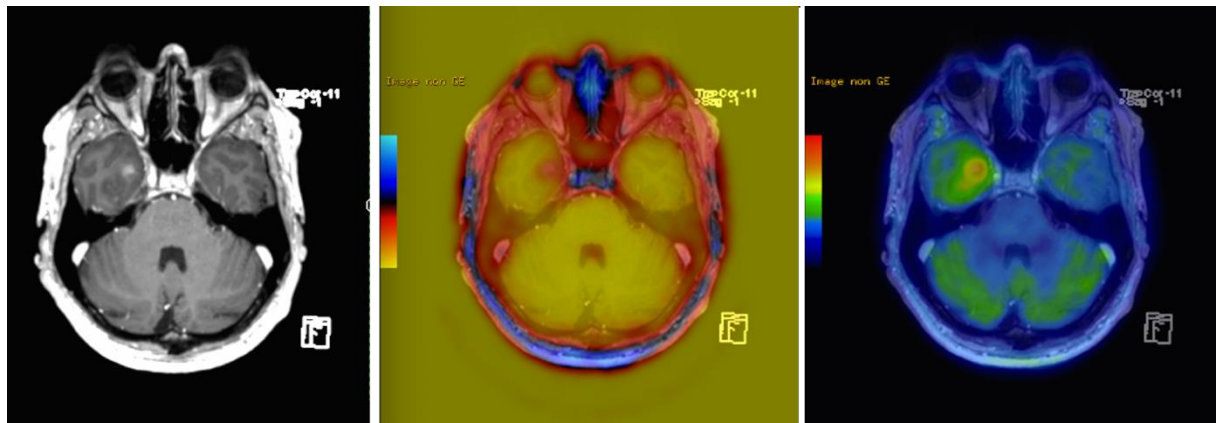
The histopathological results showed two different histologic types within the glioma in the right amygdala. The temporo-lateral and posterior temporo-median part of the tumor was infiltrated by a high-grade glioma and the anterior temporo-median part of the tumor was infiltrated by a WHO grade IV glioblastoma with small cell component.

There was another peri-lesional area in the temporo-posterior cortex lesion that showed subacute necrosis due to a post-biopsy stroke.

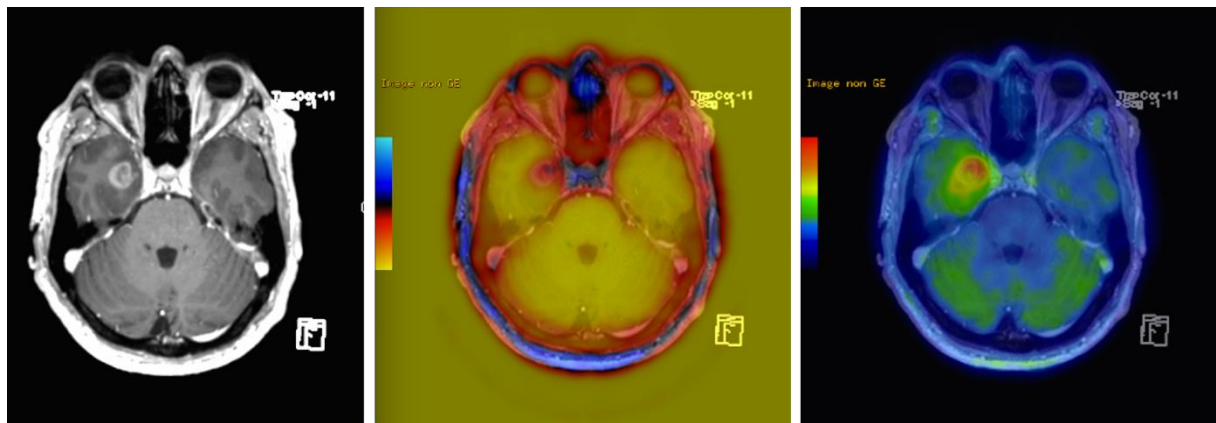
## **Patient 2:**

The histopathological results demonstrated a low-grade glioma in the right temporo-insular area with no necrosis and no endothelial proliferation. The tumor was homogenous and well defined which was typical for a glioneuronal tumor. The final report evoked a WHO grade II ganglioglioma, which will still be sent out for confirmation to a international expert site in France (result not available at the time of this report).

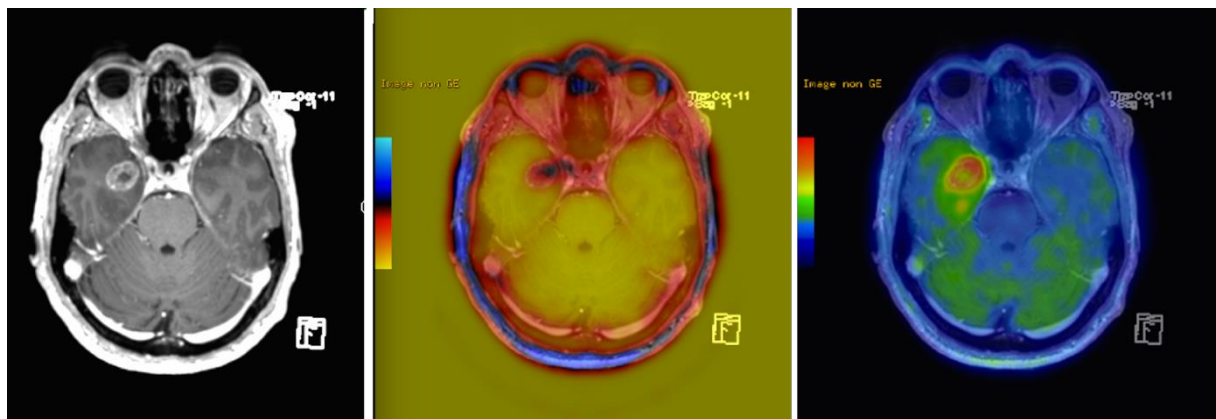
## Patient 1



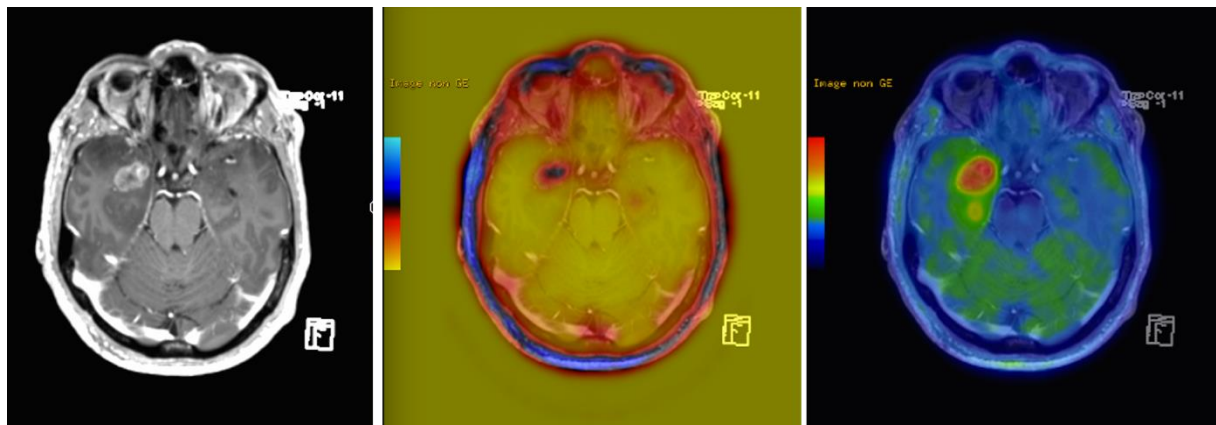
a.



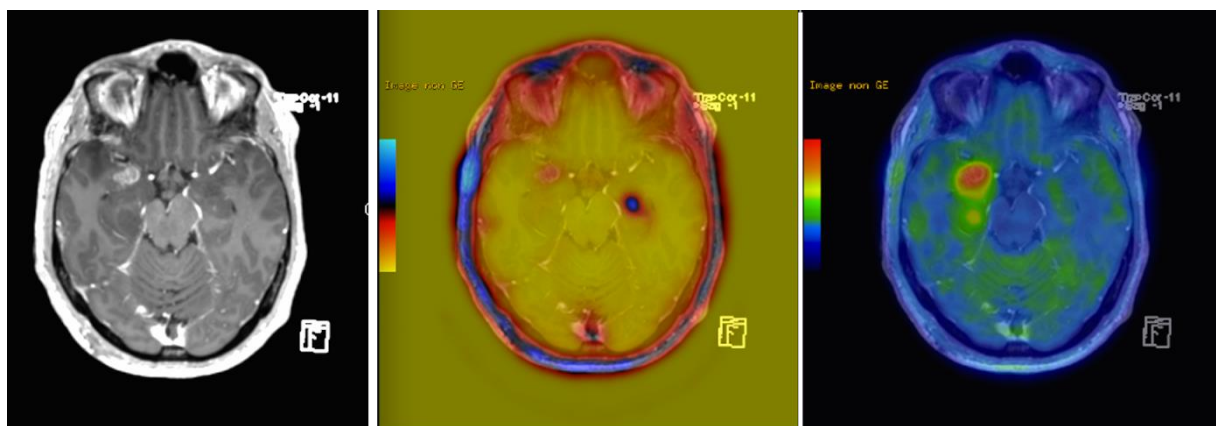
b.



c.



d.



e.

I.

II.

III.

**Figure 1** - a, b, c, d and e: trans-axial slices of a bi-component high-grade glioma/glioblastoma primary brain tumor

- I. Axial T1-weighted postgadolinium showing a hyperintense lesion in the right amygdala.
- II.  $^{68}\text{Ga}$ -NODAGA-RGD (RGD) showing uptake (SUVmax = 1.1 g/ml) in the superior antero-median side of the tumor.
- III.  $^{18}\text{F}$ -fluoro-ethyl-tyrosine (FET) PET images showing high uptake (SUVmax = 4.3 g/ml) in the temporo-polar lesion with the highest uptake in the supero-median part of the lesion.

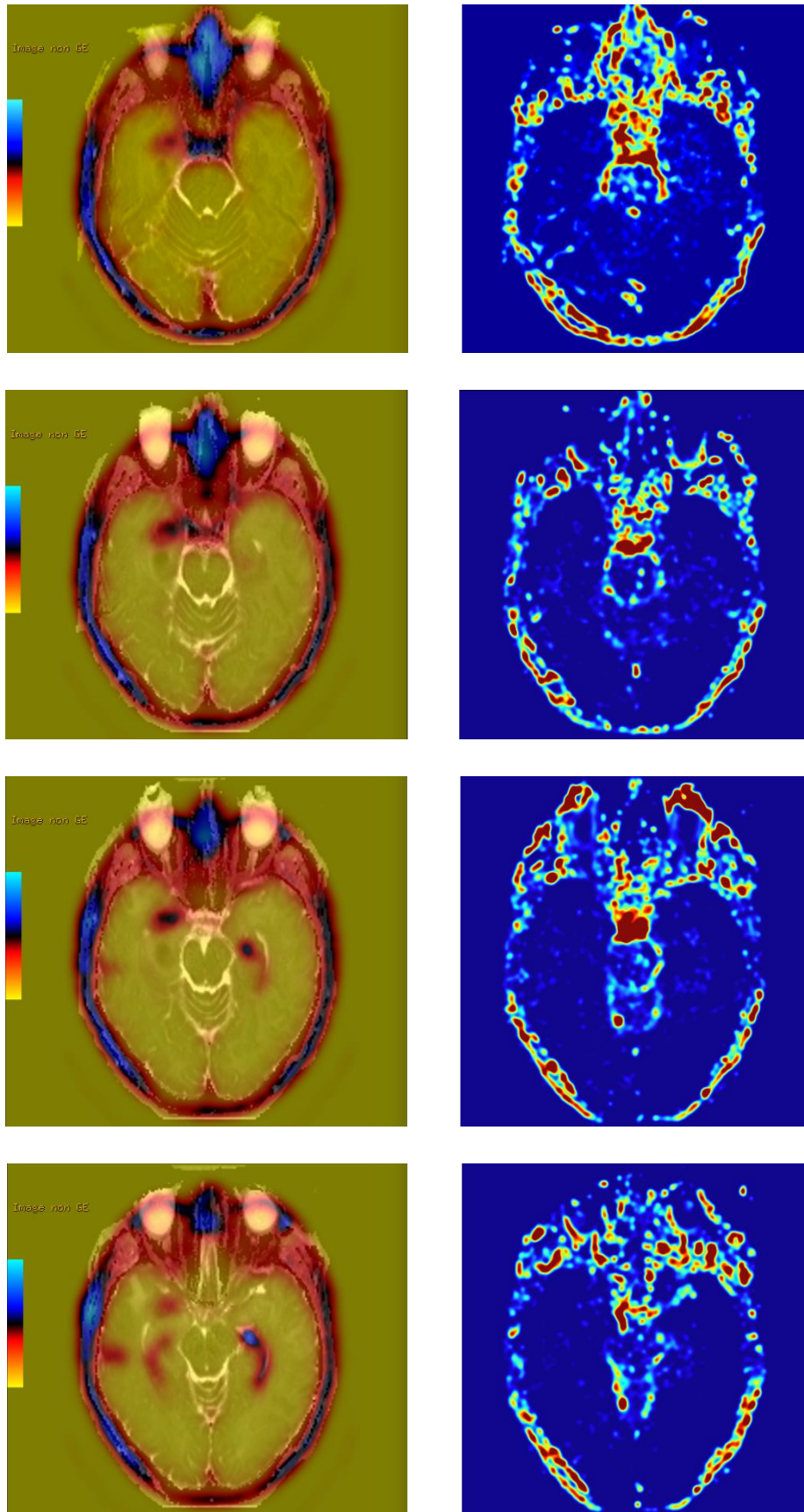


**Figure 2** - showing transaxial slices through the tumor with RGD images (left) and corresponding Intravoxel Incoherent Motion (IVIM) images (right).



## **MRI**

The MRI results showed on the postgadolinium-T1-weighted sequence, a rupture of the blood-brain barrier and contrast taken up into the temporo-polar region and right amygdala.

Moreover, there was gliomatous infiltration starting from the right amygdala and the right temporo-polar region extending to the posterior insular level with signs of high-grade transformation in the right amygdala.

## **IVIM**

On the IVIM signal images, there was visually no augmentation of cerebral microperfusion in the tumor area.

## **RGD**

PET shows uptake only in the superior and antero-median region of the tumor which corresponds according to the histopathologic results, to a grade IV glioblastoma. The SUV<sub>max</sub> in that portion of the tumor was 1.1 g/ml. The rest of the tumor shown on the MRI does not show any uptake of the tracer.

This patient has another peri-lesional captation of RGD in the right temporal area due to a post-biopsy stroke (resulting from a small-vessel peroperative hemorrhage needing coagulation) showing necrosis on the biopsy.

## **FET**

Interestingly our lesion shows a homogenous FET uptake on both anterior and posterior portion of the tumor with predominance on the supero-median region of the tumor. The SUV<sub>max</sub> in the tumor was 4.3 g/ml.

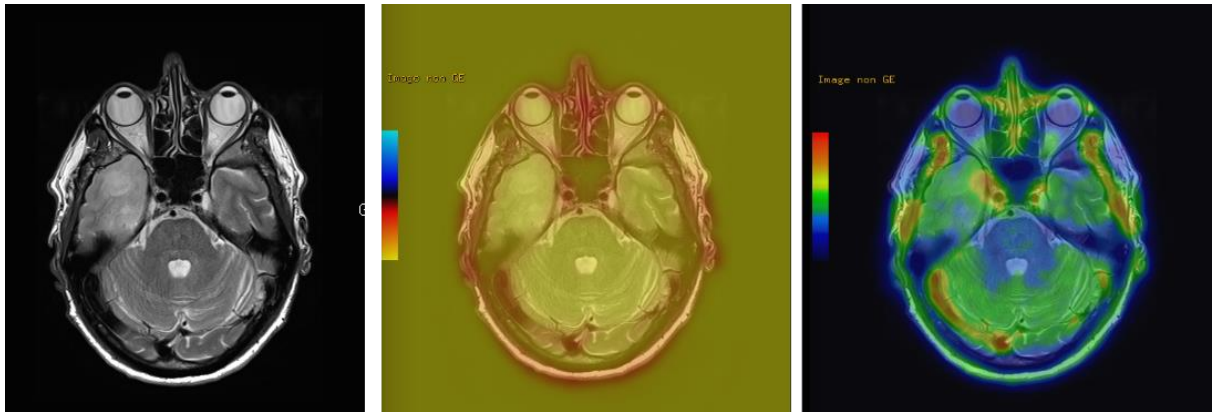
There was a another less intense site of hyperactivity posteriorly to the predominant lesion with a SUV<sub>max</sub> of 2.3 g/ml.

The tumor-to-background SUV<sub>max</sub> ratio (TBR<sub>max</sub>) was 3.1, which was consistent with a high-grade glioma according to (61) that demonstrates that a TBR<sub>max</sub> value superior to 2.0 is consistent with high grade glioma.

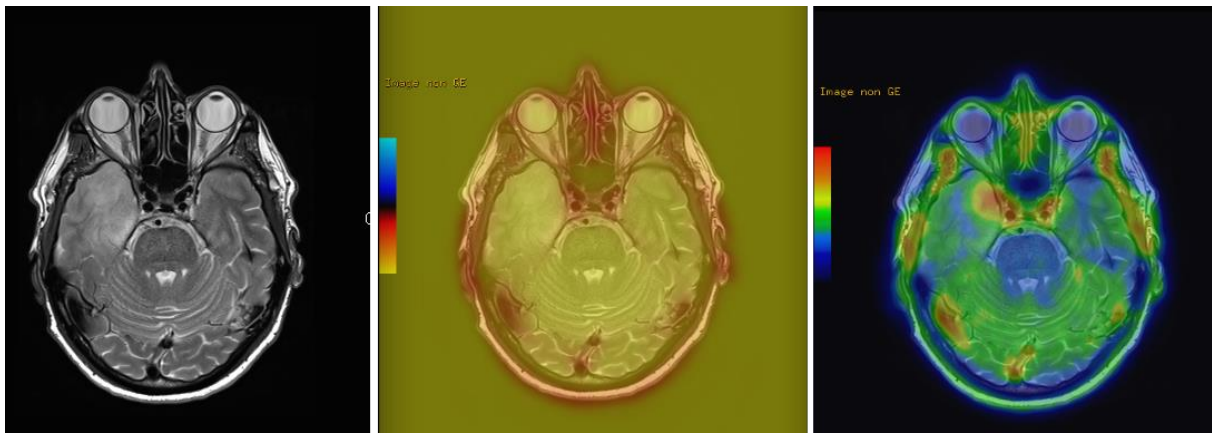
The cumulative aspect of the time-activity curve of FET uptake was evocative of a grade III-IV glioma.



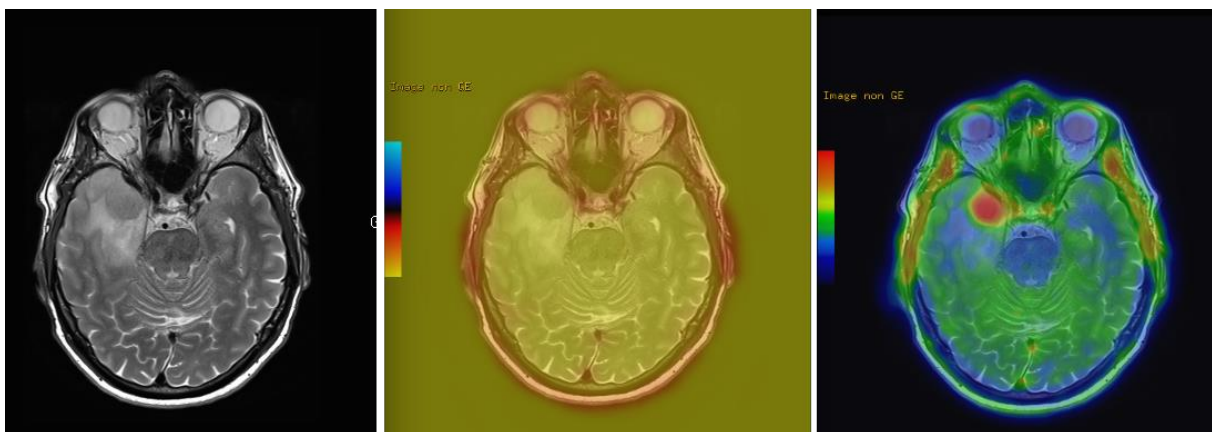
## Patient 2



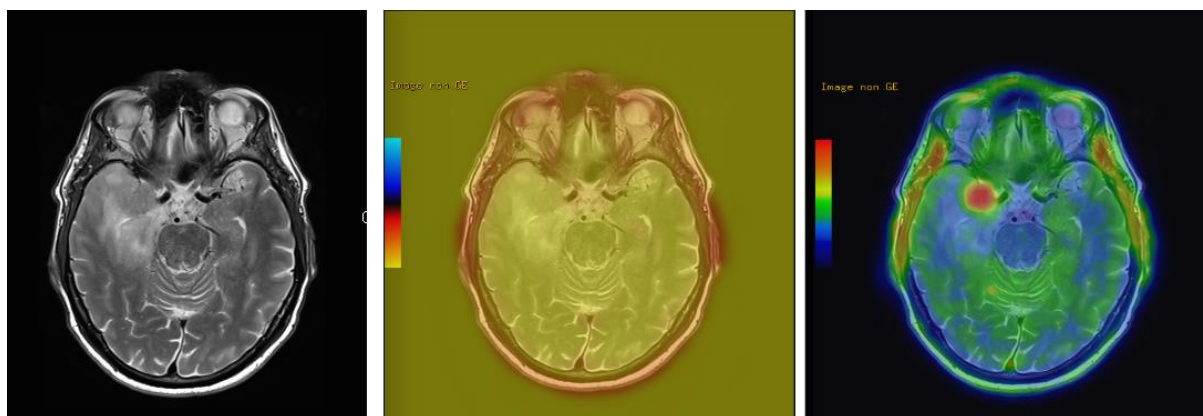
a.



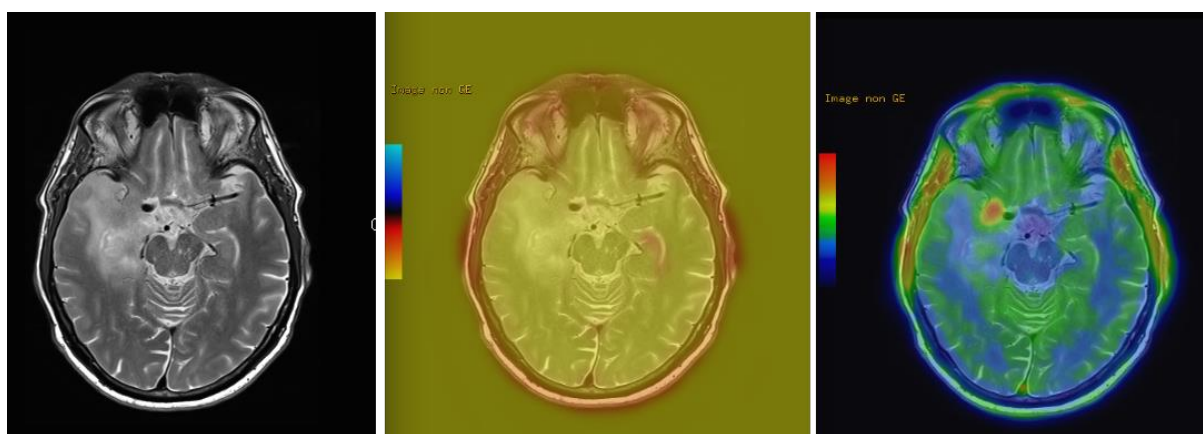
b.



c.



d.



e.

I.

II.

III.

**Figure 3** - a, b, c, d and e: transaxial slices of a WHO grade II ganglioglioma

- I.** Axial T2-weighted image showing a hyperintense lesion in the right temporo-insular region in contact with the frontal horn of the right lateral ventricle.
- II.**  $^{68}\text{Ga}$ -NODAGA-RGD showing no significant uptake in the tumor.
- III.**  $^{18}\text{F}$ -fluoro-ethyl-tyrosine (FET) PET images showing high uptake ( $\text{SUV}_{\text{max}} = 2.4 \text{ g/ml}$ ) in the right temporo-polar area.

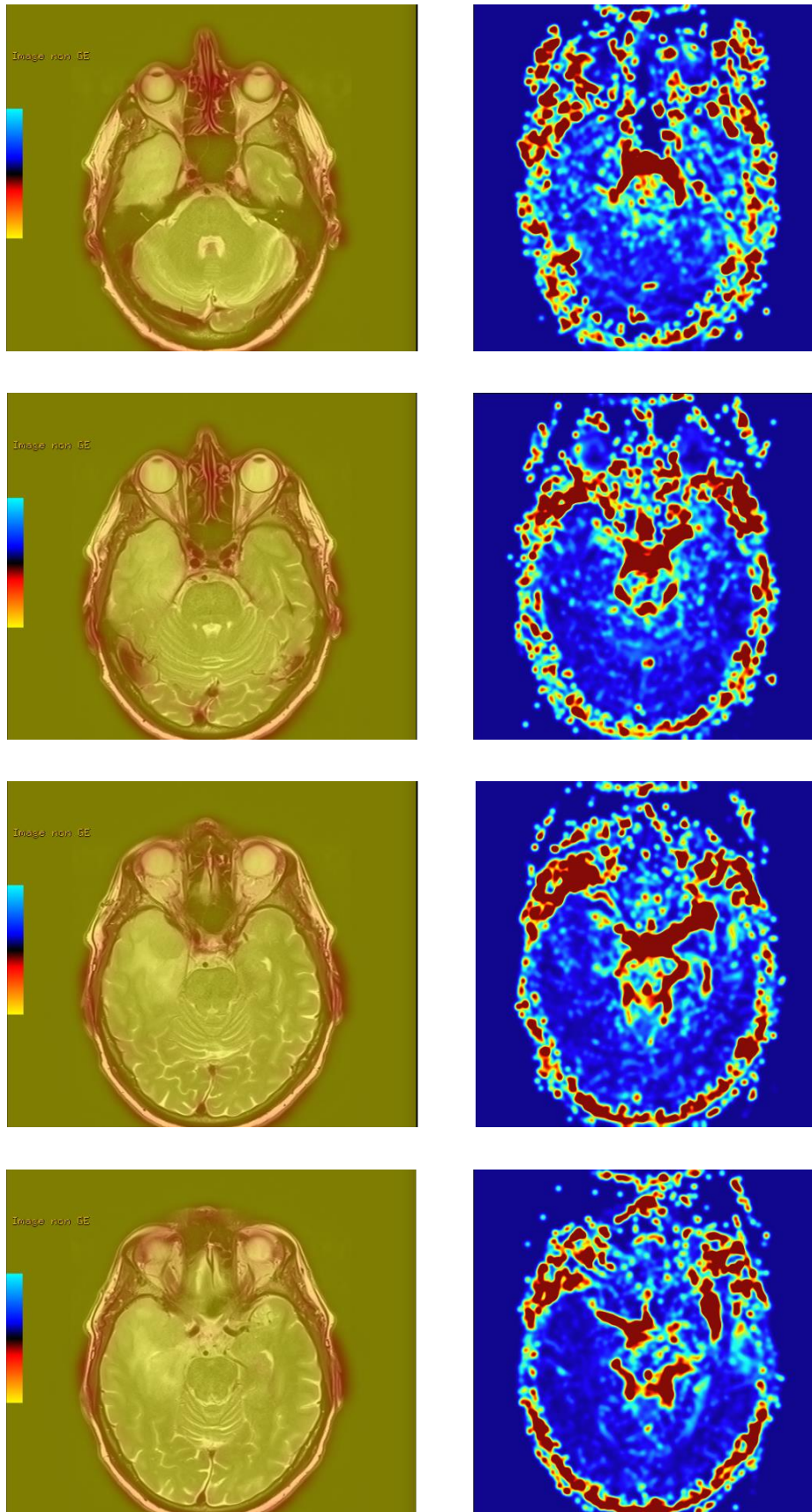


**Figure 4** - showing transaxial slices through the primary brain tumor with RGD (left) and corresponding Intravoxel Incoherent Motion (IVIM) images (right).

## **MRI**

There was no rupture of the blood-brain barrier. T2-weighted images showed a hyperintense lesion in the right temporal cortex. There was also a tumoral mass effect centered on the right temporo-polar region with infiltration consistent of a T2 signal abnormality in the amygdala, posterior hippocampus, parahippocampal gyrus and the occipito-temporal gyrus. No pathological contrast uptake was present.

## **IVIM**

Visually, the IVIM signal showed no visible augmentation of the cerebral microperfusion in the tumor area.

## **RGD**

There was no significant uptake of RGD in the cerebral tumoral region.

## **FET**

The tracer was taken up into the right temporo-polar region of the tumor with an  $SUV_{max}$  of 2.4 g/ml. There is no other suspect FET captation.

The tumor-to-background ratio max ( $TBR_{max}$ ) was 3.4 which was consistent with a high-grade glioma according to (61). In addition to that, the dynamic cumulative curve of FET uptake evokes a grade III-IV glioma.

# DISCUSSION

## RGD-FET

When we analyze the PET images of our first patient, we saw that RGD was interestingly taken up mainly into the glioblastoma portion of the tumor and also into the stroke in the posterior temporal region. Comparing the images with the histopathological slices, in patient 1, the avid part of RGD corresponded to a very vascular area with proliferative vessels according to the pathologists. The latter area corresponded to a WHO grade IV glioblastoma.

The part corresponding to a stroke was shown to have no proliferative vessels and therefore has no glioblastoma component. However, it shows a little RGD uptake, which is consistent with angiogenesis present on the post-stroke region.

The absence of RGD uptake in the posterior part of the tumor makes us suspect that there is probably no tumoral angiogenesis in that area. Indeed, that part of the tumor that showed FET uptake had no proliferative vessels according to the pathologists and therefore was not a grade IV glioblastoma. Consequently, we need to acquire more data to assess whether RGD uptake is indeed capable of differentiating between several histological types of gliomas.

For patient 2, the tumor was FET-avid, but there was no RGD uptake. The latter observation makes us think that the tumor is not very angiogenic and may not benefit from any anti-angiogenic treatment. This statement could save time by not trying an anti-angiogenic treatment and waiting until a decrease in tumor size is observed to evaluate whether the patient is responding to the therapy or not. Of course, this would need to be indeed demonstrated.

To conclude, there was a completely different uptake in our 2 patients between RGD and FET, which points up that RGD highlights a different phenomenon than FET amino-acid transport. Moreover, we need to pursue these comparisons in a larger cohort.

## **RGD-IVIM**

Apparently two different phenomena are visualized on the RGD uptake images and on the IVIM sequence.

Usually, micro-perfusion signal is higher in the glioma area (37), which interestingly was not observed in our 2 patients. The  $fD^*$  that represents cerebral perfusion volume was not higher in the tumor areas than in the rest of the brain, and this in our two cases.

The IVIM signal did not correlate with the RGD uptake in our first two patients and so far we may think that the two techniques demonstrate different processes. However, we need to include another 8 patients to finish this first comparison study and to have a better characterization of respective and cumulative values of both techniques.



## Conclusion and future work

This work is a pilot study in which RGD had yet not been compared to FET and IVIM for the evaluation of neoangiogenesis in gliomas. We noted an interesting uptake of RGD tracer in the glioblastoma region and not in the other high-grade regions of the tumor. This latter observation is consistent with a fixation of the tracer only where blood vessels are proliferating.

Our second patient did not show any RGD uptake in the tumor, nor proliferative vessels on the histopathologic slices. We could therefore emit the hypothesis that the patient would not respond to an anti-angiogenic treatment. This statement could make patients earn time in terms of survival, as they could avoid getting started on a useless anti-angiogenic treatment and be waiting for a clinical response as we know time is key in gliomas management.

As limitations, we should mention that this observation is extrapolated from one case only and that the untreated IVIM sequences are unfortunately of suboptimal quality and difficult to interpret because of the noise. This encourages us to include further patients in this study. We had difficulties including patients at the beginning of the study because of the non-reimbursement of the  $^{18}\text{F}$ -FET PET examination by the Swiss health insurances. Fortunately the latter will be reimbursed since the 1<sup>st</sup> January 2016.

To conclude, we observe three different phenomena in gliomas biology with our two cases. In order to appreciate in a more precise way the value of our RGD tracer compared to FET and IVIM, we need a larger-sized population of patients and voxel-based analysis, which is planned in the framework of my upcoming MD thesis.

Future work will consist of a comparison of the distribution of both PET tracers and two more volumes defined as:  $^{18}\text{F}$ -FET  $\cup$   $^{68}\text{Ga}$ -NODAGA-RDG and  $^{18}\text{F}$ -FET  $\cap$   $^{68}\text{Ga}$ -NODAGA-RDG with each a correlation to the IVIM signal.

Although we only have interesting preliminary results, it is difficult to establish firm conclusions with only 2 patients. However, further examination with a larger cohort would allow better understanding of RGD tracer contribution compared to the two other techniques. We will get an  $\alpha_v\beta_3$ -labeling antibody for immunofluorescence to directly correlate histopathological results with angiogenesis.

# BIBLIOGRAPHY

1. Kang CM, Koo H-J, Choe YS, Choi JY, Lee K-H, Kim B-T. 68Ga-NODAGA-VEGF121 for in vivo imaging of VEGF receptor expression. *Nucl Med Biol*. 2014 Jan;41(1):51–7.
2. Haubner R, Beer AJ, Wang H, Chen X. Positron emission tomography tracers for imaging angiogenesis. *Eur J Nucl Med Mol Imaging*. 2010 Aug;37 Suppl 1:S86–103.
3. Deshayes E, Dunet V, Rüegg C, Prior JO. Imagerie de la néoangiogenèse en médecine nucléaire. *Médecine Nucl*. 2012;36(10):619–26.
4. Iagaru A, Mosci C, Mittra E, Zaharchuk G, Fischbein N, Harsh G, et al. Glioblastoma Multiforme Recurrence: An Exploratory Study of (18)F FPPRGD2 PET/CT. *Radiology*. 2015 May 12;141550.
5. Beer AJ, Haubner R, Wolf I, Goebel M, Luderschmidt S, Niemeyer M, et al. PET-based human dosimetry of 18F-galacto-RGD, a new radiotracer for imaging  $\alpha v \beta 3$  expression. *J Nucl Med Off Publ Soc Nucl Med*. 2006 May;47(5):763–9.
6. Buchegger F, Viertl D, Baechler S, Dunet V, Kosinski M, Poitry-Yamate C, et al. 68Ga-NODAGA-RGDyK for  $\alpha v \beta 3$  integrin PET imaging. Preclinical investigation and dosimetry. *Nucl Nucl Med*. 2011;50(6):225–33.
7. Haubner R, Maschauer S, Prante O. PET radiopharmaceuticals for imaging integrin expression: tracers in clinical studies and recent developments. *BioMed Res Int*. 2014;2014:871609.
8. Dijkgraaf I, Beer AJ, Wester H-J. Application of RGD-containing peptides as imaging probes for  $\alpha v \beta 3$  expression. *Front Biosci Landmark Ed*. 2009;14:887–99.
9. Beer AJ, Haubner R, Goebel M, Luderschmidt S, Spilker ME, Wester H-J, et al. Biodistribution and pharmacokinetics of the  $\alpha v \beta 3$ -selective tracer 18F-galacto-RGD in cancer patients. *J Nucl Med Off Publ Soc Nucl Med*. 2005 Aug;46(8):1333–41.
10. Beer AJ, Schwaiger M. Imaging of integrin  $\alpha v \beta 3$  expression. *Cancer Metastasis Rev*. 2008 Dec;27(4):631–44.



11. Beer AJ, Kessler H, Wester H-J, Schwaiger M. PET Imaging of Integrin  $\alpha V\beta 3$  Expression. *Theranostics*. 2011;1:48–57.
12. Gaertner FC, Kessler H, Wester H-J, Schwaiger M, Beer AJ. Radiolabelled RGD peptides for imaging and therapy. *Eur J Nucl Med Mol Imaging*. 2012 Feb;39 Suppl 1:S126–38.
13. Beer AJ, Schwaiger M. PET imaging of  $\alpha V\beta 3$  expression in cancer patients. *Methods Mol Biol Clifton NJ*. 2011;680:183–200.
14. Haubner R, Weber WA, Beer AJ, Vabulienė E, Reim D, Sarbia M, et al. Noninvasive visualization of the activated  $\alpha V\beta 3$  integrin in cancer patients by positron emission tomography and [ $^{18}\text{F}$ ]Galacto-RGD. *PLoS Med*. 2005 Mar;2(3):e70.
15. Oxboel J, Brandt-Larsen M, Schjoeth-Eskesen C, Myschetzky R, El-Ali HH, Madsen J, et al. Comparison of two new angiogenesis PET tracers  $^{68}\text{Ga}$ -NODAGA-E[c(RGDyK)]<sub>2</sub> and  $^{64}\text{Cu}$ -NODAGA-E[c(RGDyK)]<sub>2</sub>; in vivo imaging studies in human xenograft tumors. *Nucl Med Biol*. 2014 Mar;41(3):259–67.
16. Galldiks N, Rapp M, Stoffels G, Dunkl V, Sabel M, Langen K-J. Earlier diagnosis of progressive disease during bevacizumab treatment using O-(2- $^{18}\text{F}$ -fluorethyl)-L-tyrosine positron emission tomography in comparison with magnetic resonance imaging. *Mol Imaging*. 2013 Aug;12(5):273–6.
17. Galldiks N, Langen K-J, Holy R, Pinkawa M, Stoffels G, Nolte KW, et al. Assessment of treatment response in patients with glioblastoma using O-(2- $^{18}\text{F}$ -fluoroethyl)-L-tyrosine PET in comparison to MRI. *J Nucl Med Off Publ Soc Nucl Med*. 2012 Jul;53(7):1048–57.
18. Galldiks N, Stoffels G, Filss CP, Piroth MD, Sabel M, Ruge MI, et al. Role of O-(2-( $^{18}\text{F}$ )-fluoroethyl)-L-tyrosine PET for differentiation of local recurrent brain metastasis from radiation necrosis. *J Nucl Med Off Publ Soc Nucl Med*. 2012 Sep;53(9):1367–74.
19. Galldiks N, Stoffels G, Filss C, Rapp M, Blau T, Tscherpel C, et al. The use of dynamic O-(2- $^{18}\text{F}$ -fluoroethyl)-L-tyrosine PET in the diagnosis of patients with progressive and recurrent glioma. *Neuro-Oncol*. 2015 Sep;17(9):1293–300.
20. Neuner I, Kaffanke JB, Langen K-J, Kops ER, Tellmann L, Stoffels G, et al. Multimodal imaging utilising integrated MR-PET for human brain tumour assessment. *Eur Radiol*. 2012 Dec;22(12):2568–80.
21. Senthamizhchelvan S, Zaidi H. Novel Quantitative Techniques in Hybrid (PET-MR) Imaging of Brain Tumors. *PET Clin*. 2013 Apr;8(2):219–32.

22. Henriksen OM, Larsen VA, Muhic A, Hansen AE, Larsson HBW, Poulsen HS, et al. Simultaneous evaluation of brain tumour metabolism, structure and blood volume using [(18)F]-fluoroethyltyrosine (FET) PET/MRI: feasibility, agreement and initial experience. *Eur J Nucl Med Mol Imaging*. 2015 Sep 12;
23. Filss CP, Galldiks N, Stoffels G, Sabel M, Wittsack HJ, Turowski B, et al. Comparison of 18F-FET PET and Perfusion-Weighted MR Imaging: A PET/MR Imaging Hybrid Study in Patients with Brain Tumors. *J Nucl Med*. 2014 Apr 1;55(4):540–5.
24. Beer AJ, Lorenzen S, Metz S, Herrmann K, Watzlowik P, Wester H-J, et al. Comparison of integrin  $\alpha$ V $\beta$ 3 expression and glucose metabolism in primary and metastatic lesions in cancer patients: a PET study using 18F-galacto-RGD and 18F-FDG. *J Nucl Med Off Publ Soc Nucl Med*. 2008 Jan;49(1):22–9.
25. Gempt J, Bette S, Ryang Y-M, Buchmann N, Peschke P, Pyka T, et al. 18F-fluoro-ethyl-tyrosine positron emission tomography for grading and estimation of prognosis in patients with intracranial gliomas. *Eur J Radiol*. 2015 May;84(5):955–62.
26. Dunet V, Prior JO. FET PET in Neuro-oncology and in Evaluation of Treatment Response. *PET Clin*. 2013 Apr 1;8(2):147–62.
27. Rapp M, Heinzl A, Galldiks N, Stoffels G, Felsberg J, Ewelt C, et al. Diagnostic performance of 18F-FET PET in newly diagnosed cerebral lesions suggestive of glioma. *J Nucl Med Off Publ Soc Nucl Med*. 2013 Feb;54(2):229–35.
28. Jansen NL, Graute V, Armbruster L, Suchorska B, Lutz J, Eigenbrod S, et al. MRI-suspected low-grade glioma: is there a need to perform dynamic FET PET? *Eur J Nucl Med Mol Imaging*. 2012 Jun;39(6):1021–9.
29. Dunet V, Rossier C, Buck A, Stupp R, Prior JO. Performance of 18F-Fluoro-Ethyl-Tyrosine (18F-FET) PET for the Differential Diagnosis of Primary Brain Tumor: A Systematic Review and Metaanalysis. *J Nucl Med*. 2012 Feb 1;53(2):207–14.
30. Emblem KE, Mouridsen K, Bjornerud A, Farrar CT, Jennings D, Borra RJH, et al. Vessel architectural imaging identifies cancer patient responders to anti-angiogenic therapy. *Nat Med*. 2013 Aug 18;19(9):1178–83.
31. Götz I, Grosu AL. [18F]FET-PET Imaging for Treatment and Response Monitoring of Radiation Therapy in Malignant Glioma Patients – A Review. *Front Oncol [Internet]*. 2013 [cited 2015 Jul 4];3. Available from: <http://journal.frontiersin.org/article/10.3389/fonc.2013.00104/abstract>

32. American Brain Tumor Association [Internet]. [cited 2015 Oct 23]. Available from: <http://www.abta.org/about-us/news/brain-tumor-statistics/>
33. Chen W. Clinical Applications of PET in Brain Tumors. *J Nucl Med*. 2007 Sep 1;48(9):1468–81.
34. Dunet V, Prior JO. Diagnostic accuracy of F-18-fluoroethyltyrosine PET and PET/CT in patients with brain tumor. *Clin Transl Imaging*. 2013 Apr;1(2):135–44.
35. Togao O, Hiwatashi A, Yamashita K, Kikuchi K, Mizoguchi M, Yoshimoto K, et al. Differentiation of high-grade and low-grade diffuse gliomas by intravoxel incoherent motion MR imaging. *Neuro-Oncol*. 2015 Aug 4;
36. Central Brain Tumor Registry of the United States [Internet]. [cited 2015 Oct 23]. Available from: <http://www.cbtrus.org/factsheet/factsheet.html>
37. Federau C, Meuli R, O'Brien K, Maeder P, Hagmann P. Perfusion Measurement in Brain Gliomas with Intravoxel Incoherent Motion MRI. *Am J Neuroradiol*. 2014 Feb 1;35(2):256–62.
38. Dunet V, Maeder P, Nicod-Lalonde M, Lhermitte B, Pollo C, Bloch J, et al. Combination of MRI and dynamic FET PET for initial glioma grading: *Nuklearmedizin*. 2014 Apr 16;53(4):155–61.
39. Galldiks N, Langen K-J, Pope WB. From the clinician's point of view - What is the status quo of positron emission tomography in patients with brain tumors? *Neuro-Oncol*. 2015 Nov;17(11):1434–44.
40. Gempt J, Soehngen E, Förster S, Ryang Y-M, Schlegel J, Zimmer C, et al. Multimodal imaging in cerebral gliomas and its neuropathological correlation. *Eur J Radiol*. 2014 May;83(5):829–34.
41. Metz S, Ganter C, Lorenzen S, van Marwick S, Herrmann K, Lordick F, et al. Phenotyping of tumor biology in patients by multimodality multiparametric imaging: relationship of microcirculation, alpha3 expression, and glucose metabolism. *J Nucl Med Off Publ Soc Nucl Med*. 2010 Nov;51(11):1691–8.
42. Le Bihan D, Breton E, Lallemand D, Aubin ML, Vignaud J, Laval-Jeantet M. Separation of diffusion and perfusion in intravoxel incoherent motion MR imaging. *Radiology*. 1988 Aug;168(2):497–505.
43. Le Bihan D, Breton E, Lallemand D, Grenier P, Cabanis E, Laval-Jeantet M. MR imaging of intravoxel incoherent motions: application to diffusion and perfusion in neurologic disorders. *Radiology*. 1986 Nov;161(2):401–7.
44. Le Bihan D. Intravoxel Incoherent Motion Perfusion MR Imaging: A Wake-Up Call. *Radiology*. 2008 décembre;249(3):748–52.

45. Koh D-M, Collins DJ, Orton MR. Intravoxel incoherent motion in body diffusion-weighted MRI: reality and challenges. *AJR Am J Roentgenol*. 2011 Jun;196(6):1351–61.
46. Bisdas S, Koh TS, Roder C, Braun C, Schittenhelm J, Ernemann U, et al. Intravoxel incoherent motion diffusion-weighted MR imaging of gliomas: feasibility of the method and initial results. *Neuroradiology*. 2013 Oct;55(10):1189–96.
47. Bisdas S, Klose U. IVIM analysis of brain tumors: an investigation of the relaxation effects of CSF, blood, and tumor tissue on the estimated perfusion fraction. *Magma N Y N*. 2015 Aug;28(4):377–83.
48. Federau C, O'Brien K, Meuli R, Hagmann P, Maeder P. Measuring brain perfusion with intravoxel incoherent motion (IVIM): Initial clinical experience: Brain IVIM: Initial Clinical Experience. *J Magn Reson Imaging*. 2014 Mar;39(3):624–32.
49. Hu Y-C, Yan L-F, Wu L, Du P, Chen B-Y, Wang L, et al. Intravoxel incoherent motion diffusion-weighted MR imaging of gliomas: efficacy in preoperative grading. *Sci Rep*. 2014;4:7208.
50. Bisdas S, Braun C, Skardelly M, Schittenhelm J, Teo TH, Thng CH, et al. Correlative assessment of tumor microcirculation using contrast-enhanced perfusion MRI and intravoxel incoherent motion diffusion-weighted MRI: is there a link between them? *NMR Biomed*. 2014 Oct;27(10):1184–91.
51. Lin Y, Li J, Zhang Z, Xu Q, Zhou Z, Zhang Z, et al. Comparison of Intravoxel Incoherent Motion Diffusion-Weighted MR Imaging and Arterial Spin Labeling MR Imaging in Gliomas. *BioMed Res Int*. 2015;2015:234245.
52. Federau C, Maeder P, O'Brien K, Browaeys P, Meuli R, Hagmann P. Quantitative measurement of brain perfusion with intravoxel incoherent motion MR imaging. *Radiology*. 2012;265(3):874–81.
53. Lopci E, Franzese C, Grimaldi M, Zucali PA, Navarria P, Simonelli M, et al. Imaging biomarkers in primary brain tumours. *Eur J Nucl Med Mol Imaging*. 2015 Apr;42(4):597–612.
54. Niyazi M, Jansen NL, Rottler M, Ganswindt U, Belka C. Recurrence pattern analysis after re-irradiation with bevacizumab in recurrent malignant glioma patients. *Radiat Oncol Lond Engl*. 2014;9:299.
55. Schnell O, Krebs B, Carlsen J, Miederer I, Goetz C, Goldbrunner RH, et al. Imaging of integrin  $\alpha(v)\beta(3)$  expression in patients with malignant glioma by [18F] Galacto-RGD positron emission tomography. *Neuro-Oncol*. 2009 Dec;11(6):861–70.

56. Cai H, Conti PS. RGD-based PET tracers for imaging receptor integrin  $\alpha v \beta 3$  expression. *J Label Compd Radiopharm*. 2013 May 15;56(5):264–79.
57. Beer AJ, Haubner R, Sarbia M, Goebel M, Luderschmidt S, Grosu AL, et al. Positron emission tomography using [18F]Galacto-RGD identifies the level of integrin  $\alpha v \beta 3$  expression in man. *Clin Cancer Res Off J Am Assoc Cancer Res*. 2006 Jul 1;12(13):3942–9.
58. Schnell O, Krebs B, Wagner E, Romagna A, Beer AJ, Grau SJ, et al. Expression of integrin  $\alpha v \beta 3$  in gliomas correlates with tumor grade and is not restricted to tumor vasculature. *Brain Pathol Zurich Switz*. 2008 Jul;18(3):378–86.
59. Galldiks N, Rapp M, Stoffels G, Fink GR, Shah NJ, Coenen HH, et al. Response assessment of bevacizumab in patients with recurrent malignant glioma using [18F]Fluoroethyl-L-tyrosine PET in comparison to MRI. *Eur J Nucl Med Mol Imaging*. 2013 Jan;40(1):22–33.
60. Vander Borght T, Asenbaum S, Bartenstein P, Halldin C, Kapucu O, Van Laere K, et al. EANM procedure guidelines for brain tumour imaging using labelled amino acid analogues. *Eur J Nucl Med Mol Imaging*. 2006 Nov;33(11):1374–80.
61. Dunet V, Pomoni A, Hottinger A, Nicod-Lalonde M, Prior JO. Performance of 18F-FET versus 18F-FDG-PET for the diagnosis and grading of brain tumors: systematic review and meta-analysis. *Neuro-Oncol*. 2015 Aug 4;nov148.